

1 **Isolation of highly selective IgNAR variable single-domains against a human therapeutic**
2 **Fc scaffold and their application as tailor-made bioprocessing reagents.**

3 **Magdalena J. Buschhaus^{1,2*}, Stefan Becker³, Andrew J. Porter^{1,4} and Caroline J.**
4 **Barelle¹**

5
6 ¹Elasmogen Ltd, Liberty Building, University of Aberdeen, Aberdeen AB25 2ZP, UK

7 ²Present address: UCL Cancer Institute, Paul O’Gorman Building, University College London, WC1E 6DD, UK

8 ³Merck Biopharma KGaA, Protein Engineering & Antibody Technologies, Darmstadt 64293, Germany

9 ⁴Department of Molecular and Cell Biology, Institute of Medical Sciences, University of Aberdeen, Aberdeen
10 AB25 2ZD, UK

11 *To whom correspondence should be addressed. E-mail: m.buschhaus@ucl.ac.uk
12
13

14

15

16

17

18

19

20

21

22

23

24

25

26

27

28

29

30

31 The adaptive immune system of cartilaginous fish (*Elasmobranchii*), comprising of classical
32 hetero-tetrameric antibodies, is enhanced through the presence of a naturally occurring
33 homodimeric antibody-like immunoglobulin - the new antigen receptor (IgNAR). The binding-
34 site of the IgNAR variable single-domain (VNAR) offers advantages of reduced size (<1/10th
35 of classical immunoglobulin) and extended binding topographies, making it an ideal candidate
36 for accessing cryptic epitopes otherwise intractable to conventional antibodies. These
37 attributes, coupled with high physicochemical stability and amenability to phage display,
38 facilitates selection of VNAR binders to challenging targets. Here, we explored the unique
39 attributes of these single-domains for potential application as bioprocessing reagents in the
40 development of the SEED-Fc platform, designed to generate therapeutic bispecific antibodies.
41 A panel of unique VNARs specific to the SEED homodimeric (monospecific) “by-products”
42 were isolated from a shark semi-synthetic VNAR library via phage display. The lead VNAR
43 candidate exhibited low nanomolar affinity and superior selectivity to SEED homodimer, with
44 functionality being retained upon exposure to extreme physicochemical conditions that mimic
45 their applicability as purification agents. Ultimately, this work exemplifies the robustness of
46 the semi-synthetic VNAR platform, the predisposition of the VNAR paratope to recognise
47 novel epitopes, and the potential for routine generation of tailor-made VNAR-based
48 bioprocessing reagents.

49 **Key words:** affinity ligand, SEED bispecific antibody platform, shark IgNAR, phage display,
50 variable new antigen receptor.

51

52

53

54

55

56

57

58

59

60

61 **Introduction**

62 The plethora of bispecific antibody (bsAb) formats currently in development (Spiess *et al.*
63 2015; Brinkmann and Kontermann 2017) typifies the heightened interest in these next-
64 generation biotherapeutics. In turn, this expanding multitude of bsAbs necessitates robust
65 manufacturing platforms for their unhindered progress into clinical use and on hopefully to
66 deliver both patient and commercial benefits (Liu *et al.* 2017; Shukla *et al.* 2017). High
67 expression yield is not necessarily the single most important factor for these formats, but rather
68 the efficiency with which the bsAbs form, and the corresponding presence of closely related
69 but contaminating by-products of the processes employed (e.g. monospecific binders)
70 (Brinkmann and Kontermann 2017). One molecular route to bsAbs is based on a heterodimeric
71 Fc engineering approach, to generate asymmetric mutations in each of two parental mAb CH3
72 domains (Ha *et al.* 2016). This is employed in the strand-exchange engineered domain (SEED)
73 Fc platform (Gross *et al.* 2013), and resolves the majority of the heavy chain mispairing seen
74 for other systems (Davis *et al.* 2010; Krah *et al.* 2017). This increase in efficiency is in part
75 the result of the SEED design rationale, incorporating complementary human IgG/IgA Fc
76 hybrids that are “encouraged” to preferentially heterodimerise, forming an analogue Fc
77 scaffold (Gross *et al.* 2013). Whilst the early efficacy data looks very promising, indicating a
78 favourable pharmacokinetic profile and retention of antibody-like effector functions (Muda *et*
79 *al.* 2011; Kelton *et al.* 2012), the GA chain can form low-levels of contaminating GA-GA
80 SEED homodimers (Davis *et al.* 2010). Thus far, none of the Fc heterodimeric approaches
81 have achieved 100% heterodimerisation, with low-levels (1–10%) of mispaired
82 homodimerisation being seemingly inevitable in large-scale production (Sampei *et al.* 2013;
83 Ha *et al.* 2016; Skegro *et al.* 2017). This mixed population of therapeutic scale product
84 requires, therefore, to be better characterised (or even polished) and quantifiable batch
85 consistency determined to facilitate efficient downstream bioprocessing and regulatory
86 approvals (Kufer *et al.* 2004; Ha *et al.* 2016).

87 To date, the main efforts employed to resolve this bioprocessing bottleneck have been
88 focussed on improving the manufacturability of bsAbs by further rounds of molecular
89 engineering (Sampei *et al.* 2013; Skegro *et al.* 2017). At the same time, advances in upstream
90 monoclonal antibody (mAb) processing has led to significant improvements in production
91 yields, placing even greater cost pressures on finding a suitable solution to the presence of
92 monospecific binders in the bispecific therapeutic programs (Girard *et al.* 2015).

93 For the generation of a generic approach that would work for all SEED systems the
94 recognition and/or purification challenge is not straightforward because of the close structural

95 and physicochemical resemblance of the desired heterodimeric bsAb with the by-product
96 homodimers. With only a small number of subtle differences between them in their Fc regions
97 (Shukla and Norman 2017) these changes cannot be distinguished by conventional protein A
98 capture, resulting in their co-elution (Liu *et al.* 2017). Alternative purification methods could
99 use anti-idiotypic ligands specific for intact antibody paratopes (Godar *et al.* 2015; Könning,
100 Rhiel *et al.* 2017). However elegant, such a dual anti-idiotypic purification process lacks
101 universal application, requiring an individual selection campaign for each bsAb arm.

102 Shark-derived single-domains provide opportunities as alternative affinity capture
103 reagents, sharing many similar properties to VHH domains (Wesolowski *et al.* 2009; Könning,
104 Zielonka *et al.* 2017) but superior when one considers size (up to 20% smaller), stability, and
105 density of binding loops per domain (with four regions of hypervariability versus VHH's three)
106 (Kovaleva *et al.* 2014). VNAR's distinct structural paratope (Diaz *et al.* 2002; Stanfield *et al.*
107 2004), inherent stability (Griffiths *et al.* 2013, Ubah *et al.* 2017), amenability to display
108 technologies (Ubah *et al.* 2016) and site-specific covalent coupling to crystalline nanocellulose
109 (Uth *et al.* 2014), reinforces VNAR's attractiveness.

110 VNARs were isolated from a semi-synthetic phage display library through a solution-
111 phase selection technique using biotinylated SEED Fc-based protein [N-terminal IgG1 hinge
112 region-IgG1 CH2-(SEED CH3)] in the form of 'the contaminant' SEED homodimer (Fc-
113 GA/GA-Fc) protein. A successful "candidate" affinity ligand had to demonstrate superior
114 selectivity to the target protein present at <1% of the total protein yield (~20–100 µg/mL)
115 (Davis *et al.* 2010), with the ability to differentiate between closely related mispaired formats,
116 and also show efficient elution from the target/ligand complex. In addition, the VNAR affinity
117 ligand had to be sufficiently stable to retain activity under harsh bioprocessing conditions,
118 enabling reusability without compromising performance.

119

120 **Materials and methods**

121 *Phage display selection*

122 A shark VNAR synthetic library (ELSS1, Elasmogen Ltd., patent WO/2014/173959) of
123 combined size 1×10^{11} , was selected *via* a solution-phase method (Hawkins *et al.* 1992) with
124 biotinylated SEED Fc homodimer protein: GA-GA Fc (Merck KGaA, Darmstadt Germany)
125 captured on streptavidin magnetic beads (Dynabeads M-280, Invitrogen). Clearly the purity of
126 the starting antigens is a key consideration influencing the selection of specific binders. The
127 homodimer purity (GA-GA Fc protein) was confirmed with both analytical HPLC, and
128 isoelectric focusing gel analysis that allows the amino acid composition of the AG and GA

129 SEED chains to be distinguished using different isoelectric point (pI) values (theoretical pI
130 values: AG=8.2; GA=6.4; AG/GA=7.3) (Gross *et al.* 2013). Using these approaches in
131 combination the protein was determined to be pure. For the purpose of solution-phase
132 selection, the SEED protein was biotinylated *via* EZ-Link Sulfo-NHS-LC-Biotin kit (Thermo
133 Scientific). Phage display library selections were performed using $>10^{13}$ phage/mL. Library
134 phage and Dynabeads (2x 100 μ L) were blocked with 3% (w/v) Marvel milk proteins in 1x
135 PBS (MPBS) for 1 h, rotating at room temperature. Phage were deselected on blocked beads,
136 while the remaining beads were incubated with biotinylated-SEED homodimer (200 nM) for 1
137 h rotating at room temperature. SEED pre-decorated beads were then incubated with deselected
138 phage for a further 1 h. Wash stringency was maintained at five times 1x PBS-0.05% (v/v)
139 Tween20 (PBST) and five 1x PBS, prior to an 8 min elution with 200 μ L of 100 mM
140 triethylamine, and neutralisation with 100 μ L of 1 M Tris-HCl, pH 7.5. Eluted phage output
141 was amplified through infection of 10 mL mid-log phase *Escherichia coli* (*E. coli*) TG1 cells
142 (Lucigen) for 30 min (static), at 37°C. Following infection, the cells were concentrated by
143 centrifugation, and plated on TYE agar bioassay plate containing 2% (w/v) glucose and 100
144 μ g/mL ampicillin. The phage selection output was rescued according to a previously described
145 protocol by Dooley *et al.* 2003. In brief, the selection output was scraped-off the bioassay agar
146 plate and seeded into 50 mL of 2xTY, 2% (w/v) glucose, 100 μ g/mL ampicillin media at
147 OD600 of 0.1, and grown at 37°C 250 rpm to OD600 of ~0.5. The selected phage were rescued
148 by infecting the culture with M13K07 helper phage (New England Biolabs) at 20:1 ratio
149 (phage:cells) and incubated for 30 min (static) at 37°C, followed by 1 h shaking at 150 rpm.
150 The cells were pelleted and re-suspended in 50 mL of 2xTY media containing 100 μ g/mL
151 ampicillin and 50 μ g/mL kanamycin prior to overnight incubation at 25°C, 250 rpm shaking.
152 Phage-VNAR particles were concentrated from the culture supernatant by two successive
153 precipitations with 1/5th volume of ice-cold 20% (w/v) polyethylene glycol/2.5 M NaCl with
154 30 min incubation on ice. The resulting precipitated phage were used as the input phage for
155 the next round of selection, with two further rounds of selection being carried out and
156 stringency being increased by a successive 2-fold reduction in biotinylated-SEED homodimer
157 concentration.

158 *Screening of SEED homodimer specific binders*

159 The enrichment of antigen-binding clones was evaluated *via* monoclonal phage enzyme-linked
160 immunosorbent assay (ELISA). Ninety-two individual colonies were picked from each
161 selection round and screened for binding specificity to SEED protein: GA-GA Fc homodimer,

162 AG-GA Fc heterodimer, and an unrelated human serum albumin (HSA) protein control
163 (Sigma-Aldrich), coated onto MaxiSorp ELISA plates (Thermo Fisher Scientific) at 1 µg/mL
164 in 1x PBS, 4°C overnight. Monoclonal phages were inoculated from overnight starter cultures
165 into 96-deep-well plates (Greiner Bio-One) with 800 µL/well 2xTY, 2% (w/v) glucose, 100
166 µg/mL ampicillin media, and grown with shaking at 37°C for 4 h. The phage-VNAR particles
167 were rescued by infection with M13K07 helper phage and two successive precipitations with
168 polyethylene glycol/2.5 M NaCl, as described above. Precipitated phage was added to ELISA
169 plates pre-blocked with 3% MPBS and incubated for 1 h at room temperature. Phage signals
170 were detected *via* horseradish peroxidase (HRP)-conjugated anti-M13 antibody (GE
171 Healthcare, 27-9421-01) diluted 1/1,000 in 3% MPBS for 1 h at room temperature. ELISA was
172 developed with 3,3',5,5'-tetramethylbenzidine substrate (Thermo Fisher Scientific) for 10 min
173 at room temperature and stopped with 0.5 volume of 1 M H₂SO₄, and the optical density (OD)
174 was measured at 450 nm. Plasmid DNA was prepared from antigen binding clones *via*
175 Wizard® Plus SV Minipreps DNA Purification System (Promega) for sequencing (GATC
176 Biotech).

177 *Preparation of soluble VNAR proteins*

178 Anti-SEED VNAR binders were rescued with M13K07 helper phage, and the supernatant was
179 used to infect mid-log phase HB2151 cells (a kind gift from Scotia Biologics Ltd.) for 30 min
180 at 37°C static. VNAR proteins were expressed in the cytoplasm of HB2151 cells at 1 litre scale.
181 Day cultures (TB media with 2% glucose and 100 µg/mL ampicillin) were seeded from
182 overnights at 1:50 dilution and grown for 7 h at 37°C, pellets were re-suspended in the same
183 culture volume (minus glucose) with a final concentration of 1 mM isopropyl β-D-1-
184 thiogalactopyranoside (Sigma-Aldrich) at 15°C overnight, with shaking. Cells were harvested,
185 and pellets treated with a 10% culture volume of ice-cold osmotic shock buffer: 200 mM Tris-
186 HCl, 1 mM EDTA, 20% (w/v) sucrose, pH 7.4, shaking on ice for 15 min, prior to an equal
187 volume of ice-cold 5 mM MgSO₄ then added with continued shaking for a further 15 min. The
188 supernatant was recovered containing the periplasmic extract. The VNAR soluble protein was
189 purified *via* its hexa-histidine tail using nickel ion charged immobilised metal affinity
190 chromatography agarose (Qiagen), and eluted with 500 mM imidazole, pH 8.0. Protein samples
191 were dialysed against 1x PBS, pH 7.4, before use. Protein concentration and purity was
192 determined by SDS-PAGE.

193 *Determination of binding selectivity and affinity*

194 The binding selectivity of purified VNARs was determined on ELISA plates coated with a
195 range of proteins at 1 µg/mL: both forms of SEED protein, HSA, analogue Fc scaffolds (Sigma-
196 Aldrich) in 1x PBS, 100 µL/well, overnight at 4°C, followed by 1 h blocking at room
197 temperature in 3% MPBS, 200 µL/well. Purified VNARs were added at a top concentration of
198 2.5 µg/mL and serial dilutions performed, incubated at room temperature for 1 h. The bound
199 VNARs were detected using an anti-c-Myc-HRP antibody (Roche, 11814150001).

200 Binding affinities were determined by surface plasmon resonance on a BIAcore™ T200
201 (GE Healthcare). SEED protein was immobilised onto a CM5 Series S chip (GE Healthcare)
202 in 10 mM sodium acetate pH 5.5 *via* an amine coupling kit (GE Healthcare) giving a coating
203 density of approximately 1,000 RU. A blank immobilisation was carried out for reference
204 subtraction. The purified VNAR protein was diluted in running buffer (10 mM HEPES, 500
205 mM NaCl, 0.05% Tween20, pH 7.4) to 60, 30, 15, 8, 4 and 2 nM. Each concentration was
206 injected over the immobilised ligand for 5 min at a flow rate of 30 µL/min, 20°C, and allowed
207 to dissociate for 10 min, followed by a 0.5 min regeneration with 20 mM glycine-HCl, pH 1.7.
208 The resultant sensorgrams were analysed using BIAcore™ evaluation software.

209 For the selectivity assessment on BIAcore™ T200, the VNAR F3 monomer was
210 immobilised *via* amine coupling on the chip surface Fc2, giving a coating density of 200 RU.
211 The flow channel Fc1 was used as a reference flow channel. In the interaction assay, different
212 homodimer and heterodimer concentrations present in solution were injected over the
213 immobilised ligand, and regenerated with glycine-HCl, pH 1.5.

214 *Determination of VNAR stability*

215 Thermal stability analysis was conducted using an ELISA format following published methods
216 (Dooley *et al.* 2003; Shao *et al.* 2007). To assess VNAR's ability to withstand irreversible
217 thermal denaturation, soluble VNAR protein samples at 10 µg/mL working concentration were
218 incubated for 1 h at a range of temperatures (25–100°C) on a gradient thermocycler. Following
219 heat treatment samples were allowed to cool to room temperature before analysis of binding
220 activity in an ELISA coated with SEED homodimer at 1 µg/mL. ELISA was performed using
221 1 µg/mL final concentration of VNAR protein, which was serially diluted. Residual binding
222 activity was detected with an anti-c-Myc-HRP antibody (Roche, 11814150001) and expressed
223 as a percentage of the OD value of untreated controls.

224 Similarly, pH stability of VNAR domains was determined by ELISA plates coated with
225 SEED homodimer at 1 µg/mL. VNAR proteins were prepared at a working stock of 20 µg/mL
226 in a final volume of 50 µL in 0.1 M glycine-HCl (G-HCl) at designated pH values ranging from

227 1.5-8.0. Following overnight incubation at room temperature, aliquots were withdrawn and
228 neutralised in 1x PBS (pH 7.4) to a final concentration of 1 µg/mL directly in an ELISA plate
229 and serially diluted. Active protein was detected as above.

230 A thermal shift assay, to determine VNAR's melting temperature (T_m) and structural
231 stability of the domains, was conducted (Liu *et al.* 2014). This fluorescence-based melting
232 assay made use of a StepOnePlus™ Thermocycler (Applied Biosystems) and SYPRO®
233 Orange fluorophore (Sigma-Aldrich Corp.) at a final dilution of 1:1,000 and a total of 10 µg
234 VNAR protein in a 50 µL reaction volume triplicate, prepared in 1x PBS, pH 7.4. The
235 temperature was increased from 25°C to 80°C at ~2°C/min. T_m values were obtained from
236 melting curves using the corresponding Protein Thermal Shift analysis software.

237 *Assessing VNAR's applicability as a detection reagent*

238 A sandwich ELISA format was applied to test the ability of lead VNAR F3 to detect SEED
239 homodimer present in solution, mimicking intended application as a bioprocessing reagent.
240 ELISA plate was coated overnight at 4°C with the VNAR protein as a capture ligand at 2.5
241 µg/mL in 1x PBS, 100 µL/well. SEED protein was added at top concentration of 10 µg/mL
242 and serially diluted in 1x PBS, incubated for 1 h at room temperature. Binding was detected
243 indirectly with 1/1,000 dilution of goat anti-human IgG (Fc specific) antibody (Sigma-Aldrich,
244 2136) and rabbit anti-goat IgG-HRP (Sigma-Aldrich, A8919).

245 The VNAR proteins were further evaluated for their applicability as detection reagents
246 capturing target from a heterogeneous mix of SEED proteins in solution. VNARs were
247 immobilised on an ELISA plate at a sub-saturating concentration in 1x PBS, 100 µL/well,
248 incubated overnight at 4°C. SEED proteins were pre-mixed at different proportions of
249 homodimer and heterodimer in a final combined concentration of 5 µg/mL prior to their
250 addition to a blocked ELISA plate at 100 µL/well in duplicate, then incubated for 1 h at room
251 temperature and washed as standard. Binding signal was generated following standard
252 protocols and *via* detection of bound SEED protein with a 1/200 dilution of anti-human IgG
253 (Fc specific)-HRP antibody (Sigma-Aldrich, A0170).

254 *Bio-layer interferometry analysis*

255 Determination of VNAR's applicability as a detection reagent to screen and quantify
256 contaminating levels of SEED homodimer (GA/GA) protein was performed on the Octet® QK
257 System (Pall FortéBio) with Octet Data Acquisition software 7.0. Binding association was
258 measured in 100 µL/well 1x PBS at 30°C with 1,000 rpm orbital agitation using 96-well half-

259 area black microplates (Greiner Bio-One). Anti-mouse IgG Fc capture (AMC) Dip and Read™
260 biosensors (Pall FortéBio) were pre-equilibrated in 1x PBS, pH 7.4, for 10 min. Subsequently,
261 recombinant VNAR protein containing a C-terminal-mouse IgG2a Fc fusion was loaded onto
262 biosensor tips at a concentration of 80 µg/mL for 200 s. Followed by 60 s wash in 1x PBS.
263 Association was performed using SEED homodimer (GA/GA) Fc protein at 150 µg/mL and 75
264 µg/mL for 100 s.

265 *pH elution ELISA*

266 An ELISA-elution assay was adapted from (Kummer and Li-Chan 1998), as a screening tool
267 to test the dissociation of the VNAR-SEED complex and to compare the effectiveness of
268 eluents. ELISA plates were coated with F3 VNAR protein at 2.5 µg/mL in 1x PBS, 100 µL/well
269 overnight at 4°C. A total of 100 µL of SEED homodimer protein at a concentration of 5 µg/mL
270 in 1x PBS was applied to the wells and incubated at room temperature for 1 h. The eluent used
271 in this study was 0.1 M glycine-HCl (G-HCl), which is a standard eluent for IgG purification,
272 and the effectiveness of a range of pH 1.5–8.0 on dissociation was assessed. Each elution buffer
273 was applied at a volume of 100 µL/well: once, twice or three times, with incubation periods at
274 room temperature of 20 min each. The SEED protein remaining after elution was detected
275 indirectly with anti-human IgG (Fc specific) (Sigma-Aldrich, I2136) and anti-goat-HRP
276 (Sigma-Aldrich, A8919) conjugate diluted 1/1,000 in 3% MPBS. The potential denaturing
277 effects of the eluents were also monitored, where the integrity of the VNAR was examined by
278 testing subsequent re-binding to SEED homodimer protein.

279 *Site-directed biotinylation of VNAR domains*

280 For the purpose of site-directed biotinylation of VNAR F3 monomer, commercially available
281 Expresso® Biotin Cloning and Expression System (Lucigen) was used as per manufacturer's
282 instructions. To evaluate the capture of SEED protein from solution, biotinylated VNAR F3
283 protein was immobilised on streptavidin magnetic Dynabeads M-280 for 30 min at room
284 temperature, rotating at 20 rpm. The depleted supernatant was collected through magnetic rack
285 pull-down and the beads were washed with 1 mL 1x PBS, upon which 50 µL of 100 µg/mL
286 SEED protein either homodimer or heterodimer was added to the pelleted beads for re-
287 suspension and incubated for 1 h at room temperature, rotating at 20 rpm. Finally, the
288 supernatant was collected by pelleting the beads on a magnetic rack, and re-suspending the
289 beads in 50 µL 1x PBS. Both supernatant and beads were reduced and analysed on SDS-PAGE,

290 and Western blot *via* anti-human IgG (Fc specific)-HRP (Sigma-Aldrich, A0170) (1:1,000
291 dilution) to detect captured SEED protein.

292 *Reformatting and transient expression of VNAR as Fc fusion*

293 Plasmid DNA encoding VNAR F3 was isolated *via* Wizard® Plus SV Minipreps DNA
294 Purification System (Promega), cloned into pEEE2A mouse IgG2a Fc vector (Elasmogen Ltd.)
295 through restriction *Bss*HIII and *Bsi*WI cloning and transformed into electrocompetent *E. coli*
296 XL1-Blue cells (Agilent Technologies). Once the DNA sequence was confirmed, plasmid
297 DNA from individual clones was extracted *via* Qiagen Plasmid Midi Kit for PEI-mediated
298 transfection and transient expression in HEK293 host cells (Huh *et al.* 2007; Backliwal *et al.*
299 2008) using serum free FreeStyle™ 293 media (Invitrogen). Purification of expressed protein
300 was achieved by protein A affinity chromatography (ProSep Ultra Plus Protein A, Millipore).
301 To the harvested supernatant, 1/10th volume of 1 M Tris-HCl buffer (pH 8.0) and 5 M NaCl
302 was added and mixed thoroughly before adding 1.5 mL protein A resin per 100 mL culture.
303 The suspension was kept rotating at 15 rpm for 3 h at room temperature. The resulting resin
304 was washed 3x with 1x PBS and loaded onto gravity flow Poly-Prep® columns (Bio-Rad
305 Laboratories). VNAR-Fc fusion protein was eluted using 8 mL 0.1 M G-HCl buffer, pH 3.0,
306 and the eluate neutralised with 2 mL 1 M Tris-HCl buffer, pH 8.0. The eluate was buffer
307 exchanged into 1x PBS through dialysis (Snake Skin® dialysis tubing 7 kDa MWCO, Thermo
308 Fisher Scientific) against 1 L 1x PBS/1 mL eluted protein, pH 7.4, overnight at 15°C, followed
309 by further 5 h dialysis in fresh 1x PBS and finally concentrated using Amicon® Ultra-15
310 Centrifugal Filters (MWCO 10 kDa). Protein quality was assessed *via* SDS-PAGE and
311 quantified using Ultrospec™ 6300 pro UV/Visible Spectrophotometer (Amersham Bioscience)
312 taking an absorbance reading at 280 nm wavelength.

313 For kinetic analysis of VNAR fusions, SEED ligand was immobilised at approximately
314 1,000 RU on a CM5 series S chip in 10 mM sodium acetate, pH 5.5. The purified F3-Fc fusion
315 protein and the F3 monomer were diluted separately in running buffer to final concentrations
316 of 250, 125, 62.5, 31.25, 15.63, 7.82, 3.91, 1.95 and 0 nM at 25°C. Each concentration was
317 injected over immobilised ligand for 5 min at a constant flow rate of 30 µL/min and allowed to
318 dissociate for 10 min, followed by a 30 s regeneration pulse with 20 mM glycine, pH 1.7, at 30
319 µL/min, 240 s stabilisation period and a 50 mM NaOH wash. Reference subtracted sensorgrams
320 for each concentration were analysed.

321 **Results**

322 *Selection of single-domains specific to SEED homodimer*

323 With the aim of isolating antigen-specific shark-derived single-domain binders *via* phage
324 display, a synthetic VNAR phage library ELSS1 (Elasmogen Ltd., patent WO/2014/173959)
325 was panned against biotinylated SEED target captured on streptavidin magnetic beads. The
326 method of antigen presentation was a key influencer on the selection outcome. To more closely
327 mimic natural target presentation (Verheesen *et al.* 2003) this solution-based method biased
328 outcomes towards the isolation of binders to soluble forms of the target proteins. Three rounds
329 of affinity selections were carried out against SEED homodimer target, with a 2-fold reduction
330 in antigen concentration from round 2 included, to help drive the isolation of target specific
331 high-affinity binders. Enrichment was evaluated *via* monoclonal phage ELISA against the
332 selection target: SEED homodimer and a control protein, HSA. A high proportion of ELISA-
333 positive clones with $OD_{450\text{ nm}} \geq 0.5$ (as determined by ELISA cut-off) were isolated after the
334 third round of selection (Figure 1a). No binding to HSA was observed. Furthermore, individual
335 clones from round 3 phage were assessed for SEED selectivity by ELISA (Figure 1b), and
336 specifically their ability to distinguish between the two forms of the SEED protein, homodimer
337 and heterodimer formats.

338 *Sequence analysis of selected clones*

339 Sequence analysis identified only four unique homodimer-specific leads which may indicate
340 the rarity of binders capable of distinguishing between two such closely related antigens.
341 Whilst several hundred clones were screened, only 20 clones (less than 1%) were sequenced
342 based on their binding profile meeting the following criteria: (i) a “strong” positive (above 0.5
343 O.D) binding signal *via* phage ELISA, (ii) confirmatory binding of the same clones after
344 soluble protein was released (but not purified) from the bacterial periplasm and (iii) negative
345 on the control heterodimer antigen. Out of these 20 clones; 4 had frameshifts when sequenced,
346 F3 appeared 3 times out of the remaining 16 sequences, and C3; 5 out of 16, E4 and A4
347 appeared once. In total 8 unique clones were identified however the remaining 4 clones were
348 considered positive but weak binders as soluble protein.

349 Unique binding sequences were aligned using the clustalW method in MegAlign
350 DNASTAR Lasergene12 software and deduced amino acid sequences (Figure 2a) with
351 variations limited to within the CDR1 and CDR3 regions. Interestingly, despite the theoretical
352 sequence diversity of the synthetic library (100 billion unique clones), two homodimer specific
353 binders, E4 and C3, shared the same CDR1 sequence. Sequence analysis also established that
354 these selected VNARs were either of type IIb or IIIb IgNAR genes that lacked non-canonical

355 cysteines residues and maintained a tryptophan (W) residue in CDR1, typical of type IIIb
356 isotypes (Kovaleva *et al.* 2014), and which is a significant proportion of the ELSS1 library.
357 Canonical cysteines were maintained in frameworks 1 and 3b (Streltsov *et al.* 2004) to stabilise
358 the VNAR fold (ribbon representation, Figure 2b).

359 *VNAR characterisation: specificity and affinity*

360 To demonstrate that the lead VNAR domains were capable of selective binding to SEED
361 homodimer, and also lacked cross-reactivity to analogues Fc scaffolds, the VNAR leads were
362 expressed as soluble protein to allow functional characterisation in the absence of phage
363 particles. Recombinant VNARs were harvested from *E. coli* cell periplasm and purified by
364 nickel affinity chromatography *via* the hexa-histidine tail. The specificity of antigen binding
365 was determined by ELISA *via* anti-c-Myc-HRP detection. All four clones showed superior
366 binding to SEED homodimer with no reactivity to other related Fc domains including: SEED
367 heterodimer, IgG or IgA from human sera or IgG from sera of other species: mouse, rat, sheep,
368 rabbit (Figure 3).

369 The choice of a lead candidate was prioritised on the basis of the greatest affinity and
370 optimal binding kinetics for the SEED homodimer. Using these criteria, clone F3 was selected
371 as it exhibited the most favourable binding kinetics, quantified with surface plasmon resonance
372 analysis by BIAcore™ (Figure 4), with overall affinity in the low nM range (Table 1).

373 ***Evaluation of VNAR domain applicability as diagnostic and purification reagents***

374 *SEED selectivity in solution*

375 Recombinant VNARs were tested for their ability to capture SEED in a sandwich ELISA
376 (Figure 5), with the ELISA set-up mimicking affinity purification (i.e. where VNAR is
377 immobilised and SEED is present in solution). The F3 clone performed well as a capture
378 reagent, demonstrating its ability to bind SEED homodimer (Figure 5a) whilst maintaining no
379 reactivity to the heterodimer analogue (Figure 5b).

380 *VNAR F3 characterisation: stability assessment*

381 A key deliverable from this study was to assess the utility of isolated SEED binders as
382 (reusable) affinity purification reagents using pH changes to modify elution conditions. VNAR
383 F3 could tolerate a wide range of pH 1.5-8.0 using 0.1 M G-HCl eluent (Figure 6a), a crucial
384 characteristic for the reusability of any purification resin. The ability of purified F3 VNAR
385 protein to withstand irreversible thermal denaturation during a short (1 h) incubation period at
386 elevated temperature was also investigated. Upon heat exposure to a range of temperatures, F3

387 protein was serially diluted and assessed for binding functionality in ELISA. The percentage
388 binding activity in comparison to controls held at room temperature was calculated and the
389 values were plotted in Figure 6b. Approximately 90% activity was retained at the top VNAR
390 concentration up to 50°C, with a progressive drop in activity observed at higher temperatures.
391 This correlated well with F3's melting temperature of ~50°C as determined by the thermal shift
392 assay (Figure 6c).

393 *pH elution efficacy*

394 An ELISA-elution assay was devised as a screening tool for quantifying dissociation efficiency
395 of the VNAR-antigen complex. The effect of one, increasing to three, washes with 0.1 M G-
396 HCl as eluent, at a range of pHs from 1.5–8.0 on the dissociation of VNAR F3 bound to SEED
397 homodimer protein was quantified (Figure 7a). As a control these ELISA absorbance values
398 were compared to washes with 1x phosphate buffered saline (1x PBS) (pH 7.4). G-HCl eluent
399 at pH 1.5 resulted in the most effective elution profile even after a single treatment exposure,
400 with dissociation also observed at pH 2.0 and 3.0. The integrity of the VNAR protein and its
401 re-binding functionality to SEED homodimer following exposure to eluents was tested by
402 reapplying the homodimer protein post elution (Figure 7b).

403 *VNAR F3 functionalised streptavidin beads as SEED homodimer-specific capturing* 404 *agents*

405 To further assess the potential application of VNAR F3 as a purification reagent, the lead
406 candidate was biotinylated to facilitate immobilisation on a solid support. In order to avoid
407 generation of heterogeneous products that may occur through chemical biotinylation, a site-
408 directed approach with a C-terminal Avi tag sequence, was used facilitating *in vivo* site-
409 directed biotinylation exploiting the *E. coli* biotin ligase (BirA).

410 The ability to recover either SEED homodimer or heterodimer proteins from solution
411 was determined using capture by streptavidin magnetic beads pre-decorated with biotinylated
412 VNAR F3, and analysed *via* SDS-PAGE (Figure 8a). The streptavidin beads were heated in
413 loading buffer to release the biotinylated protein from streptavidin prior to gel analysis.
414 Consequently, some streptavidin was also released from the resin yielding a protein band
415 migrating between 10 and 15 kDa. Specific capture of SEED homodimer from solution *via*
416 bead-immobilised biotinylated-VNAR F3 was also evaluated by Western blot through
417 detection of captured protein using an anti-human IgG (Fc specific)-HRP conjugate (Figure
418 8b).

419 *Affinity enhancement through Fc reformatting*

420 One could imagine a situation where the lead F3 domain is used in certain instances as both an
421 affinity capture reagent and a diagnostic (ELISA) reagent. In an attempt to increase the
422 functional affinity, and in turn the utility of the domain as a diagnostic tool, the VNAR F3
423 monomer was reformatted as a mouse IgG2a Fc fusion construct, to generate a bivalent binder
424 that should benefit from an avidity effect whilst at the same time offering an alternative
425 immobilisation approach *via* Fc-capture. The VNAR F3-Fc was expressed transiently in a
426 eukaryotic HEK293 system. Purification of the VNAR-fusion protein was achieved *via* protein
427 A affinity chromatography using a suitable gravity-flow column. Protein quality was assessed
428 *via* SDS-PAGE (Figure 9a) and indicated a highly purified VNAR F3-Fc with bands migrating
429 between 40 kDa and 50 kDa, consistent with the predicted molecular weight. The concentration
430 of the expressed protein was determined on an Ultrospec™ 6300 pro UV/Visible
431 spectrophotometer (Amersham Bioscience, GE Healthcare) and confirmed a yield of
432 approximately 4.5 mg per litre of cell culture. A small but noteworthy increase in apparent
433 binding affinity, through an uplift in avidity (decreased off-rate), was achieved as kinetic
434 assessment on the BIAcore™ of the F3 monomer versus F3-Fc fusion resulted in a decrease in
435 K_D from 1.5 nM to 0.6 nM, using the SEED homodimer as an immobilised ligand (Table 2).
436 No binding to heterodimer protein being observed (Figure 9b).

437 The ability of the F3 lead to differentiate between SEED homodimer and heterodimer
438 proteins in a heterogeneous solution mix was tested to determine the approximate limit of
439 detection for the homodimer contaminant. The sandwich-based ELISA employed,
440 demonstrated VNAR's ability to specifically capture SEED homodimer in a concentration-
441 dependent manner from a heterogeneous mix of SEED proteins (Figure 10). Increasing the
442 heterodimer protein % did not contribute to the binding signal. The modest increase in affinity
443 measure for the F3-Fc format did indeed appear to increase the sensitivity of this new reagent
444 in an ELISA format with the bivalent F3-Fc capable of quantifying SEED homodimer
445 contaminants in the mixture when they are only 2.5% of the total SEED protein, corresponding
446 to 125 ng/mL.

447 *Applicability of VNAR F3 for target detection using bio-layer interferometry and surface*
448 *plasmon resonance*

449 The VNAR F3-Fc fusion was assessed *via* bio-layer interferometry on an Octet® QK System
450 (Pall FortéBio), testing its possible applicability as an “in-line” biosensor detection reagent
451 with signal generated using anti-mouse IgG Fc capture. The immobilised VNAR-Fc construct

452 demonstrated a concentration-dependent binding to SEED homodimer protein present in
453 solution (Figure 11a). Surface plasmon resonance studies further validated the overall superior
454 selectivity of the parental VNAR ligand as it was also able to detect and quantify the
455 contaminating presence of SEED homodimer in a heterogeneous mixture of SEED proteins
456 (Figure 11b).

457 **Discussion**

458 The central aim of this project was to explore the utility of shark-derived single domain binders
459 as bioprocessing reagents, and in particular determine their ability to remove an important
460 processing bottleneck in the development of “scaled-up” SEED bispecific therapeutics. The
461 combination of shark-derived VNAR domains and phage-display is a well-trodden route to the
462 successful isolation of specific binders to an ever-growing list of targets (Nuttall *et al.* 2001;
463 Nuttall *et al.* 2002; Dooley *et al.* 2003; Liu *et al.* 2007; Liu, Anderson and Goldman 2007;
464 Shao *et al.* 2007; Ubah *et al.* 2017). The potential applicability of camelid VHH single-domains
465 as bioprocessing and affinity capture reagents (Detmers *et al.* 2010) and biosensors (Bever *et*
466 *al.* 2016) have been previously reviewed. Of particular relevance to this program of work,
467 Klooster and colleagues (2007) isolated two IgG specific VHHs from an immune phage display
468 library. These specifically recognised all four human IgG isotypes with nanomolar affinities
469 (3–6 nM) through binding to the relatively conserved CH1 domain within the Fab region. This
470 technology was subsequently commercialised under the name CaptureSelect™ IgG-CH1
471 affinity matrix (Thermo Fischer Scientific) for human IgG purification, with a binding capacity
472 of 25–30 g IgG/L (Kruljec and Bratkovič 2017). GE Healthcare commercialised another
473 camelid-based affinity ligand directed this time against the human constant domain of the λ
474 light chain. This LambdaFabSelect affinity matrix was designed for Fab antibody fragment
475 purification with a binding capacity of 12 g Fab/L.

476 The growing list of commercially available VHH-based affinity resins sets the scene
477 for the, as yet, unexplored application of shark-derived single-domains as bioprocessing
478 reagents. Whilst they share many similar properties with VHH domains at ~11 kDa, VNARs
479 are the smallest naturally occurring binding domains in the vertebrate kingdom (Stanfield *et al.*
480 2004), and therefore possess a much higher density of binding loops by size, with four regions
481 of hypervariability contributing to specificity (Kovaleva *et al.* 2014). Their small size
482 combined with their amenability to modular reformatting and biomaterials conjugation
483 (Kovaleva *et al.* 2014; Barelle and Porter 2015; Nogueira *et al.* 2019) offers the potential of

484 multivalent arrangements for enhanced avidity as well as promoting high surface density
485 formats leading to increased binding capacity.

486 Interestingly, previous screens with scFv libraries failed to isolate binders capable of
487 distinguishing between hetero and homodimer forms of the SEED protein (pers. commun.,
488 results not shown). VHH libraries have not been screened, but their success with other IgG
489 domains would suggest that they may also provide a source of discriminatory clones.

490 The VNAR phage display library used as the starting material for this project was
491 designed to contain extended CDR3 loops, ranging from 9–26 amino acids and typically longer
492 than those found in the variable domains of mice or humans (Diaz *et al.* 2002). In addition,
493 the paratope of VNARs containing these extended CDRs appear pre-disposed to access
494 pockets, grooves and protein clefts present on the surface of target proteins. These cryptic
495 epitopes (such as enzyme binding sites) (Stanfield *et al.* 2004), are rarely “seen” by more
496 conventional antibodies which have a much more planar binding site, made up from variable
497 heavy and light domains.

498 Two requirements essential for the usefulness of an affinity ligand are: (i) binding
499 specificity to target protein and (ii) effective elution of target from the ligand complex (with
500 the possible added bonus of reusability) (Verheesen *et al.* 2003; Tu *et al.* 2015). VNARs were
501 isolated using solution-phase selection techniques with biotinylated SEED homodimer protein
502 captured on magnetic streptavidin beads. This solution-phase strategy was chosen to encourage
503 the recognition of the soluble form of the SEED protein. Four leads were specific for SEED
504 homodimer and lacked reactivity to other Fc scaffolds (human, mouse, rat) including the SEED
505 heterodimer.

506 These results demonstrate VNAR’s exquisite ability to access and recognise differences
507 between closely related and sterically restricted conformational epitopes most probably within
508 the CH3-CH3 interface. In the absence of a co-crystal structure, we can only speculate where
509 this homodimer specific domain binds, but it is unlikely to be a linear peptide as this would
510 tend to promote cross-reactivity with the heterodimeric (AG-GA) construct sharing the GA
511 CH3 domain. It is also unlikely that it binds outside of the SEED CH3 domain, such as the
512 hinge region or the CH2 domain, as here again it is hard to see how discrimination between the
513 two closely related proteins could be achieved. It seems sensible to postulate that a
514 combination of their reduced size and protruding CDR3 loop (average loop length of lead
515 clones was 11 residues) enabled them to recognise the target molecule’s surface topology.
516 Indeed, these characteristics of a VNAR paratope appears to predispose access to recessed
517 epitopes otherwise intractable to the relatively flat binding surfaces of conventional mAbs

518 (Stanfield *et al.* 2004; Stanfield *et al.* 2007; Henderson *et al.* 2007) as well as discontinuous
519 anti-idiotypic epitopes (Könning, Rhiel *et al.* 2017). With an average length of 11 amino acids
520 the VNAR CDR3 loops of the lead clones are well within the CDR3 lengths seen in mammals,
521 and so it might be sensible to conclude that the “finger-projection” positioning of the VNAR
522 CDR3 may be even more important than simple loop length alone (Stanfield *et al.* 2004;
523 Kovalenko *et al.* 2013).

524 The affinity of this interaction was determined *via* surface plasmon resonance analysis
525 on BIAcore™ and one clone in particular, F3, had a single digit nanomolar affinity of 1.6 nM
526 for homodimer and without measurable cross-reactivity to the closely related heterodimer
527 protein. Whilst there are a few absolute affinities of VNARs reported in the literature, this high
528 affinity was actually better than others previously published from a naïve spiny dogfish semi-
529 synthetic CDR3 mutagenised library of 10.2 ± 7.2 nM for staphylococcal enterotoxin B target
530 (Liu, Anderson and Goldman 2007) and was closer to the sub-nanomolar affinity (0.7–0.9 nM)
531 reported for a VNAR isolated from an immunised spiny dogfish-derived library against human
532 serum albumin (Müller *et al.* 2012). This further emphasises the robustness of this non-
533 immunised synthetic VNAR phage display (combinatorial) platform, which combines the
534 isolation of high affinity binders with a predisposition to recognise cryptic epitopes.

535 One additional characteristic of the VNAR domains is their inherent ability to tolerate
536 non-physiological (denaturing) conditions and again highlights their utility as a possible (and
537 reusable) immunoaffinity reagent. IgNAR’s naturally reside in the harsh environment of shark
538 serum consisting of high salt (1 osmolar) and high urea (350–500 mM) (Dooley *et al.* 2006;
539 Stanfield *et al.* 2007; Trischitta *et al.* 2012). The F3 clone, in particular, retained functionality
540 after overnight exposure to extremes of pH (pH 1.5–8.0) typically used for elution and
541 regeneration of affinity resins (Verheesen *et al.* 2003; Wang *et al.* 2013), with retention of
542 binding activity of $99.9 \pm 1.4\%$ and $92.4 \pm 2\%$ respectively.

543 Similarly, clone F3 exhibited high thermal stability, retaining $55.6 \pm 0.1\%$ binding
544 activity following 1 h incubation at 80°C and correlated well with previous stability
545 assessments of VNARs (Dooley *et al.* 2003; Liu, Anderson and Goldman 2007; Goodchild *et al.*
546 *et al.* 2011), and VHH’s which has achieved <60% binding recovery after heat-induced unfolding
547 in the range of 65–84°C (Dumoulin *et al.* 2002), and contrasted with conventional murine-
548 derived variable fragments and mAbs which were fully inactivated (irreversibly denatured)
549 following 50°C and 70°C incubations, respectively (Goodchild *et al.* 2011). Even after boiling
550 at 100°C for 1 h, VNAR F3 retained $14.1 \pm 1\%$ binding activity to the SEED protein. VNAR
551 protein architecture appears to encourage rapid refolding when returned to physiological

552 conditions facilitated by their simple single-chain Ig structure, which unlike conventional
553 antibodies presents a considerable number of exposed hydrophilic surface residues, as well as
554 stabilising intra-molecular disulphide bridges (Stanfield *et al.* 2004; Streltsov *et al.* 2004).

555 The VNAR's apparent ability to selectively recognise SEED protein in solution
556 indicates its potential as a sensitive and specific reagent for on-line diagnostic applications. A
557 capture assay using VNAR F3-functionalised magnetic beads showed VNAR's applicability
558 in this format. VNAR-Fc capture *via* anti-mouse IgG Fc capture Dip and Read™ biosensors in
559 conjunction with bio-layer interferometry on the Octet® QK System further confirmed the
560 functional interaction with the GA/GA SEED homodimer present in solution. This setup being
561 an optimal Octet® format for screening cell culture supernatants with SEED protein free in
562 solution, and functioning as a proof of concept of VNAR's intended on-line application as a
563 SEED homodimer detection reagent.

564 Enhancement of binding reactivity of the single binding domain was achieved through
565 multimerisation (Ubah *et al.* 2017), with dimerisation in the literature often resulting in as much
566 as a 10-fold higher affinity than monomeric domains (Simmons *et al.* 2006). The homodimer
567 specific VNAR F3 was reformatted as a mouse IgG2a Fc fusion, which allowed for
568 dimerisation through Fc-mediated association whilst at the same time offering an alternative
569 immobilisation approach *via* Fc-capture. The reformatted VNAR F3 domain demonstrated an
570 enhanced affinity (K_D) to 0.6 nM, and this was attributed to a modest avidity effect. This 2.5-
571 fold improvement over the parental monomeric construct was brought about by a 7.5-fold
572 slower dissociation rate constant (k_d). The enhanced affinity of the bivalent VNAR-reagent
573 also translated into an improved sensitivity to target in a sandwich-based ELISA, and so whilst
574 this delivered a relatively small enhancement in assay sensitivity from 500 ng/mL to 125 ng/mL
575 for SEED homodimer protein detection, this could eventually be an important format for on-
576 line diagnostic applications.

577 The VNAR F3 clone could also be used for affinity purification with regeneration of
578 the reagent being an important and desirable property, and ideally comparable to protein A
579 resin reusability of >100 purification cycles (Wang *et al.* 2013; Tu *et al.* 2015). The stability
580 assessment data from these studies certainly confirmed VNAR's ability to withstand overnight
581 exposure to pH 1.5 without any detrimental effects in its binding capacity. The effect of eluent
582 treatment on the VNAR's integrity and ability to rebind SEED was assessed in an ELISA-
583 based elution assay, with a good stability profile observed following the first elution cycle.
584 However, F3's binding capacity was slowly diminished following consecutive cycles of elution
585 at low pH range (1.5–2.0), but importantly stability was retained at pH 3.0, which is a typical

586 elution condition used in affinity purification. No stripping of immobilised VNAR from the
587 ELISA wells was detected, suggesting that its robustness and biological inactivity could make
588 the VNAR ligand a superior and safer alternative to protein A, which has been associated with
589 safety concerns related to stripping of protein A from columns and resulting risk of product
590 contamination (Low *et al.* 2007). These initial findings imply that further optimisation, for
591 instance by means of engineering pH-dependant binding through the generation of a histidine-
592 doped F3 sub-library (Könning *et al.* 2016) or the addition of a stress engineering step during
593 the selection process for enhanced stability (Pershad and Kay 2013) may be desirable in a final
594 product. In a pH stability test designed to mimic the environment of the gut, comparing anti-
595 hTNF- α VNAR and VHH binding activity following exposure to pH 3.0 over extended periods,
596 concluded that both domain scaffolds retained activity (around 80%) after 28 days. This
597 compared with a mAb which retained only 1.6% following 21 days exposure, when the
598 experiment was stopped (Ubah *et al.* 2017).

599 In conclusion, we have explored the utility of shark-derived single-domain VNARs as
600 diagnostic and affinity reagents for targets that have proved intractable to more typical
601 antibody-based technologies. Phage display selection was successful in delivering SEED
602 homodimer specific VNAR domains with low nanomolar affinity, despite only subtle interface
603 differences between SEED GA/GA and AG/GA heterodimer protein, with further affinity and
604 sensitivity enhancement achieved upon dimerisation. In addition, VNAR's exceptional
605 stability and resistance to irreversible denaturation marks VNAR domains as promising affinity
606 capturing agents for a range of purification applications.

607 **Acknowledgements**

608 The authors would like to thank Iris Willenbücher and Kerstin Hallstein for the BIAcore™
609 analysis, and Nadine Barron for the bio-layer interferometry work. This work was supported
610 by the Industrial Biotechnology Innovation Centre, and Merck KGaA.

611 **References**

- 612 Backliwal,G., Hildinger,M., Hasija,V. and Wurm,F.,M. (2008) *Biotechnol. Bioeng.*, **99**, 721-
613 727.
- 614 Barelle,C. and Porter,A. (2015) *Antibodies*, **4**, 240-258.
- 615 Bever,C.S., Dong,JX., Vasylieva, N., Barnych,B., Cui,Y., Xu,ZL., Hammock,B.D. and
616 Gee,S.J. (2016) *Anal. Bioanal. Chem.*, **408**, 5985–6002.

- 617 Brinkmann,U. and Kontermann,R.E. (2017) *mAbs*, **9**, 182-212.
- 618 Choe,W., Durgannavar,T.A. and Chung,S.J. (2016) *Materials*, **9**, 94.
- 619 Davis,J.H., Aperlo,C., Li,Y.,Kurosawa,E., Lan,Y., Lo,K.M. and Huston,J.S. (2010) *Protein*
620 *Eng. Des. Sel.*, **23**, 195-202.
- 621 Detmers,F., Hermans,P., Jiao,J. and and McCue,J. (2010) *Bioprocess Int.*, **8**, 50-54.
- 622 Diaz,M., Stanfield,R., Greenberg,A. and Flajnik,M. (2002) *Immunogenetics*, **54**, 501-512.
- 623 Dolk,E., van der Vaart,M., Hulsik,D., Vriend,G., de Haard,H., Spinelli,S., Cambillau,C.,
624 Frenken,L. and Verrips,T. (2005) *Appl. Environ. Microbiol.*, **71**, 442-450.
- 625 Dooley,H., Flajnik,M. and Porter,A. (2003) *Mol. Immunol.*, **40**, 25-33.
- 626 Dooley,H., Stanfield,R.L., Brady,R.A. and Flajnik,M.F. (2006) *Proc. Natl. Acad. Sci. U. S. A.*,
627 **103**, 1846-1851.
- 628 Dumoulin,M., Conrath,K., Van Meirhaeghe,A., Meersman,F., Heremans,K., Frenken,L.,
629 Muyldermans,S., Wyns,L. and Matagne,A. (2002) *Protein Sci.*, **11**, 500-515.
- 630 Eifler,N., Medaglia,G., Anderka,O., Laurin,L. and Hermans,P. (2014) *Biotechnol. Prog.*, **30**,
631 1311-1318.
- 632 Girard,V., Hilbold,N.J., Ng,C.K., Pegon,L., Chahim,W., Rousset,F. and Monchois,V. (2015)
633 *J. Biotechnol.*, **213**, 65-73.
- 634 Godar,M., Morello,V., Sadi,A., Hultberg,A., De Jonge,N., Basilico,C., Hanssens,V.,
635 Saunders,M., Lambrecht,B.N., El Khattabi,M., de Haard,H., Michieli,P. and Blanchetot,C.
636 (2016) *Sci. Rep.*, **6**, 31621.
- 637 Goodchild,S.A., Dooley,H., Schoepp,R.J., Flajnik,M. and Lonsdale,S.G. (2011) *Mol.*
638 *Immunol.*, **48**, 2027-2037.
- 639 Griffiths,K., Dolezal,O., Parisi,K., Angerosa,J., Dogovski,C., Barraclough,M., Sanalla,A.,
640 Casey,J.L., González,I., Perugini,M.A., Nuttall,S. and Foley,M. (2013) *Antibodies*, **2**, 66-81.
- 641 Gross,A.W., Dawson,J.P., Muda,M., Kelton,C., McKenna,S.D. and Hock,B. (2013) In
642 Schmidt,S.R. (ed), *Fusion Protein Technologies for Biopharmaceuticals: Applications and*
643 *Challenges*. John Wiley & Sons, Inc., Hoboken, NJ, USA, pp. 557-569.
- 644 Ha,J., Kim,J. and Kim,Y. (2016) *Front. Immunol.*, **7**, 394.
- 645 Hawkins,R., Russell,S. and Winter,G. (1992) *J. Mol. Biol.*, **226**, 889-896.
- 646 Henderson,K.A., Streltsov,V.A., Coley,A.M., Doleza,O., Hudson,P.J., Batchelor,A.H.,
647 Gupta,A., Bai,T., Murphy,V.J., Anders,R.F., Foley,M. and Nuttall,S.D. (2007) *Structure*, **15**,
648 1452-1466.

- 649 Huh,S.H., Do,H.J., Lim,H.Y., Kim,D.K., Choi,S.J., Song,H., Kim,N.H., Park,J.K.,
650 Chang,W.K., Chung,H.M. and Kim,J.H. (2007) *Biologicals*, **35**, 165-171.
- 651 Kelton,C., Wesolowski,J.S., Soloviev,M., Schweickhardt,R., Fischer,D., Kurosawa,E.,
652 McKenna,S.D. and Gross,A.W. (2012) *Arch. Biochem. Biophys.*, **526**, 219-225.
- 653 Klooster,R., Maassen,B.T.H., Stam,J.C., Hermans,P.W., ten Haaft,M.R., Detmers,F.J.M., de
654 Haard,H.J., Post,J.A. and Verrips, C.T. (2007) *J. Immunol. Methods*, **324**, 1-12.
- 655 Könning,D., Zielonka,S., Grzeschik,J., Empting,M., Valldorf,B., Krah,S., Schröter,C.,
656 Sellmann,C., Hock,B. and Kolmar,H. (2017) *Curr. Opin. Struct. Biol.*, **45**, 10-16.
- 657 Könning,D., Zielonka,S., Sellmann,C., Schröter,C., Grzeschik,J., Becker,S. and Kolmar,H.
658 (2016) *Mar. Biotechnol.*, **18**, 161-167.
- 659 Könning,D., Rhiel,L., Empting,M., Grzeschik,J., Sellmann,C., Schröter,C., Zielonka,S.,
660 Dickgießer,S., Pirzer,T., Yanakieva,D., Becker,S. and Kolmar,H. (2017) *Sci. Rep.*, **7**, 9676.
- 661 Kovalenko,O.V., Olland,A., Piché-Nicholas,N., Godbole,A., King,D., Svenson,K.,
662 Calabro,V., Müller,M.R., Barelle,C.J., Somers,W., Gill,D.S., Mosyak,L. and Tchistiakova,L.
663 (2013) *J. Biol. Chem.*, **288**, 17408-17419.
- 664 Kovaleva,M., Ferguson,L., Steven,J., Porter,A. and Barelle,C. (2014) *Expert Opin. Biol. Ther.*,
665 **14**, 1527-1539.
- 666 Krah,S., Sellmann,C., Rhiel,L., Schröter,C., Dickgiesser,S., Beck,J., Zielonka,S., Toleikis,L.,
667 Hock,B., Kolmar,H. and Becker,S. (2017) *N. Biotechnol.*, **29**, 167-173.
- 668 Kruljec,N. and Bratkovič,T. (2017) *Bioconjug. Chem.*, **28**, 2009-2030.
- 669 Kufer,P., Lutterbuse,R. and Baeuerle,P.A. (2004) *Trends Biotechnol.*, **22**, 238-244.
- 670 Kummer,A. and Li-Chan,E. (1998) *J. Immunol. Methods*, **211**, 125-137.
- 671 Ladenson,R.C., Crimmins,D.L., Landt,Y. and Ladenson,J.H. (2006) *Anal. Chem.*, **78**, 4501-
672 4508.
- 673 Liu,H., Saxena,A., Sidhu,S.S. and Wu,D. (2017) *Front. Immunol.*, **8**, 38.
- 674 Liu,J.L., Anderson,G.P., Delehanty,J.B., Baumann,R., Hayhurst,A. and Goldman,E.R. (2007)
675 *Mol. Immunol.*, **44**, 1775-1783.
- 676 Liu,J.L., Anderson,G.P. and Goldman,E.R. (2007) *BMC Biotechnol.*, **7**, 78.
- 677 Low,D., O'Leary,R. and Pujar,N.S. (2007) *J. Chromatogr. B Analyt. Technol. Biomed. Life*
678 *Sci.*, **848**, 48-63.
- 679 Muda,M., Gross,A.W., Dawson,J.P., He,C., Kurosawa,E., Schweickhardt,R., Dugas,M.,
680 Soloviev,M., Bernhardt,A., Fischer,D., Wesolowski,J.S., Kelton,C., Neuteboom,B. and
681 Hock,B. (2011) *Protein Eng. Des. Sel.*, **24**, 447-454.

- 682 Müller,M.R., Saunders,K., Grace,C., Jin,M., Piche-Nicholas,N., Steven,J., O'Dwyer,R.,
683 Wu,L., Khetemenee,L., Vugmeyster,Y., Hickling,T.P., Tchistiakova,L., Olland,S., Gill,D.,
684 Jensen,A. and Barelle,C.J. (2012) *mAbs*, **4**, 673-685.
- 685 Nogueira,J.C.F., Greene,M.K., Richards,D.A., Furby,A.O., Steven,J., Porter,A., Barelle,C.,
686 Scott,C.J and Vijay Chudasama. (2019) *Chem. Commun.*, **55**, 7671-7674.
- 687 Nuttall,S.D., Krishnan,U.V., Doughty,L., Nathanielsz,A., Ally,N., Pike,R.N., Hudson,P.J.,
688 Kortt,A.A. and Irving,R.A. (2002) *FEBS Lett.*, **516**, 80-86.
- 689 Nuttall,S.D., Krishnan,U.V., Hattarki,M., De Gori,R., Irving,R.A. and Hudson,P.J. (2001) *Mol.*
690 *Immunol.*, **38**, 313-326.
- 691 Pershad.K. and Kay,B.K. (2013) *Methods*, **60**, 38-45.
- 692 Sampei,Z., Igawa,T., Soeda,T., Okuyama-Nishida,Y., Moriyama,C., Wakabayashi,T.,
693 Tanaka,E., Muto,A., Kojima,T., Kitazawa,T., Yoshihashi,K., Harada,A., Funaki,M.,
694 Haraya,K., Tachibana,T., Suzuki,S., Esaki,K., Nabuchi,Y. and Hattori,K. (2013) *PLoS One*, **8**,
695 e57479. doi:10.1371/journal.pone.0057479.
- 696 Shao,C.Y., Secombes,C.J. and Porter,A.J. (2007) *Mol. Immunol.*, **44**, 656-665.
- 697 Shukla,A. and Norman,C. (2017) In Gottschalk,U. (ed), *Process scale purification of*
698 *antibodies*. John Wiley & Sons, Inc., Hoboken, NJ, USA, pp. 559-595.
- 699 Shukla,A., Wolfe,L., Mostafa,S. and Norman,C. (2017) *Bioeng. Transl. Med.*, **2**, 58-69.
- 700 Simmons,D.P., Abregu,F.A., Krishnan,U.V., Proll,D.F., Streltsov,V.A., Doughty,L.,
701 Hattarki,M.K. and Nuttall,S.D. (2006) *J. Immunol. Methods*, **315**, 171-184.
- 702 Skegro,D., Stutz,C., Ollier,R., Svensson,E., Wassmann,P., Bourquin,F., Monney,T., Gn,S. and
703 Blein,S. (2017) *J. Biol. Chem.*, **292**, 9745-9759.
- 704 Spiess,C., Zhai,Q. and Carter,P.J. (2015) *Mol. Immunol.*, **67**, 95-106.
- 705 Stanfield,R.L., Dooley,H., Verdino,P., Flajnik,M.F. and Wilson,I.A. (2007) *J. Mol. Biol.*, **367**,
706 358-372.
- 707 Stanfield,R., Dooley,H., Flajnik,M. and Wilson,I. (2004) *Science*, **305**, 1770-1773.
- 708 Streltsov,V.A., Varghese,J.N., Carmichael,J.A., Irving,R.A., Hudson,P.J. and Nuttall,S.D.
709 (2004) *Proc. Natl. Acad. Sci. U.S.A.*, **101**, 12444-12449.
- 710 Trischitta,F., Faggio,C. and Torre,A. (2012) *OJAS.*, **2**, 32-40.
- 711 Tu,Z., Xu,Y., Fu,J., Huang,Z., Wang,Y., Liu,B. and Tao,Y. (2015) *J. Chromatogr. B Analyt.*
712 *Technol. Biomed. Life Sci.*, **983**, 26-31.
- 713 Ubah,O.C., Steven,J., Kovaleva,M., Ferguson,L., Barelle,C., Porter,A.J.R. and Barelle,C.J.
714 (2017) *Front. Immunol.*, **8**, 1780.

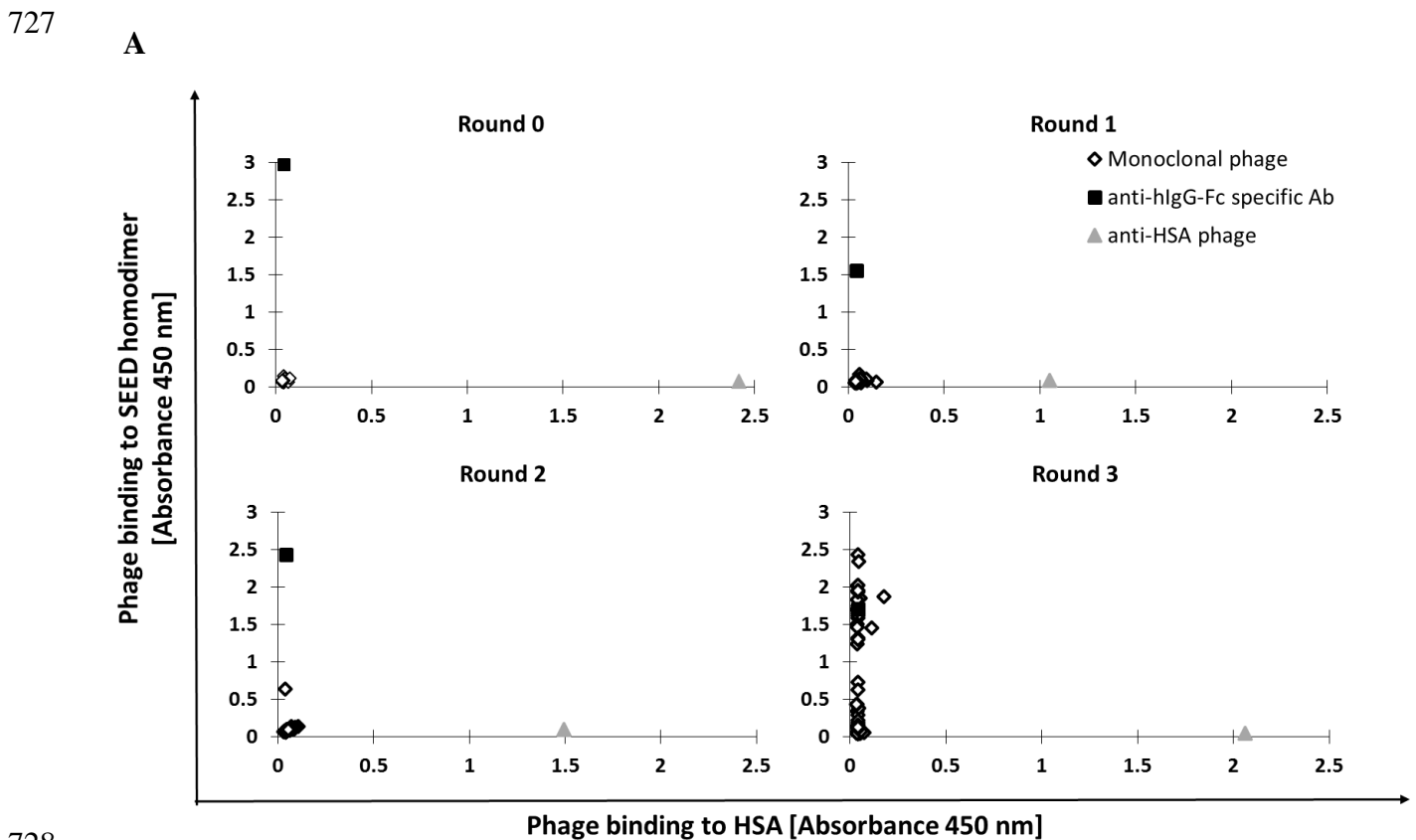
715 Ubah,O.C., Barelle,C.J., Buschhaus,M.J. and Porter,A.J. (2016) *Curr. Pharm. Des.*, **22**, 6519-
716 6526.

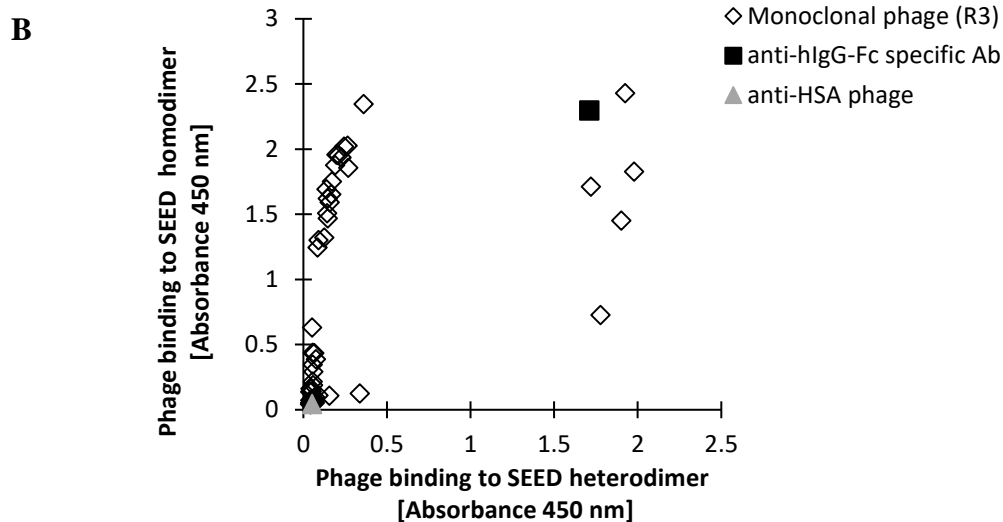
717 Uth,C., Zielonka,S., Hörner,S., Rasche,N., Plog,A., Orelma,H., Avrutina,O., Zhang,K. and
718 Kolmar,H. (2014) *Angew. Chem. Int. Ed. Engl.*, **53**, 12618-12623.

719 Verheesen,P., Ten Haaft,M.R., Lindner,N., Verrips,C.T. and De Haard,J.J.W. (2003) *Biochim.*
720 *Biophys. Acta*, **1624**, 21-28.

721 Wang,L., Dembecki,J., Jaffe,N.E., O'Mara,B.W., Cai,H., Sparks,C.N., Zhang,J., Laino,S.G.,
722 Russell,R.J. and Wang,M. (2013) *J. Chromatogr. A*, **1308**, 86-95.

723 Wesolowski,J., Alzogaray,V., Reyelt,J., Unger,M., Juarez,K., Urrutia,M., Cauerhff,A.,
724 Danquah,W., Rissiek,B., Scheuplein,F., Schwarz,N., Adriouch,S., Boyer,O., Seman,M.,
725 Licea,A., Serreze,D.V., Goldbaum,F.A., Haag,F. and Koch-Nolte,F. (2009) *Med. Microbiol.*
726 *Immunol.*, **198**, 157-174.

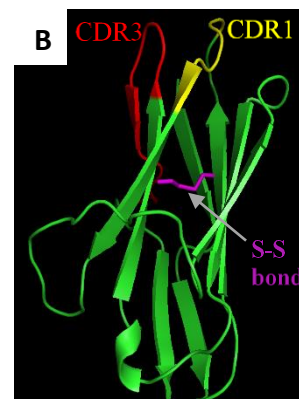
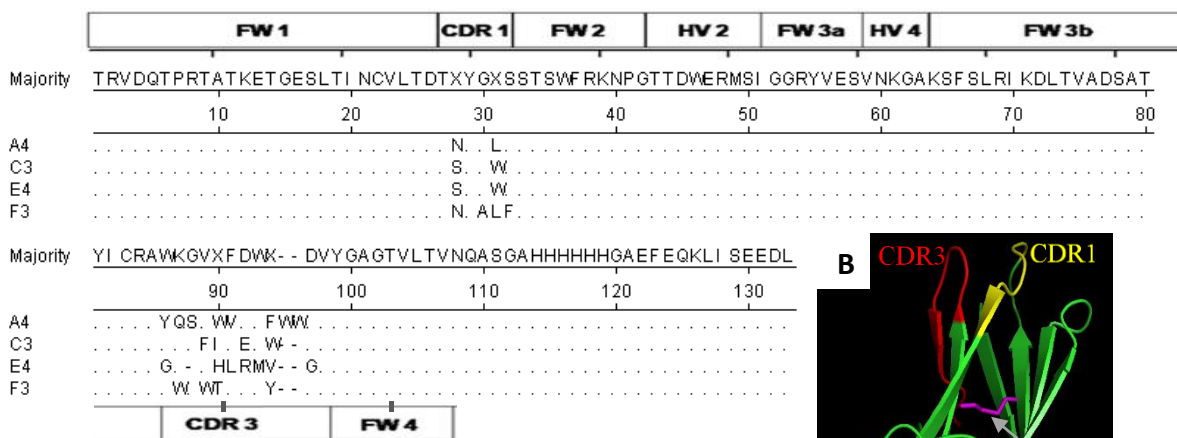




729

730 **Fig. 1.** Round specific monoclonal phage ELISA. (A) Monoclonal phage ELISA evaluating 92
 731 clones at each round of selection. Each point represents a single clone tested for binding to
 732 either the target SEED homodimer, or irrelevant control HSA. (B) Round 3 phage monoclonal
 733 ELISA assessing binding selectivity to SEED homodimer versus SEED heterodimer. Positive
 734 binders are defined as an absorbance 450 nm reading of ≥ 0.5 . Relevant positive controls
 735 included: anti-HSA phage, anti-human IgG (Fc specific)-HRP antibody control for SEED
 736 coating.

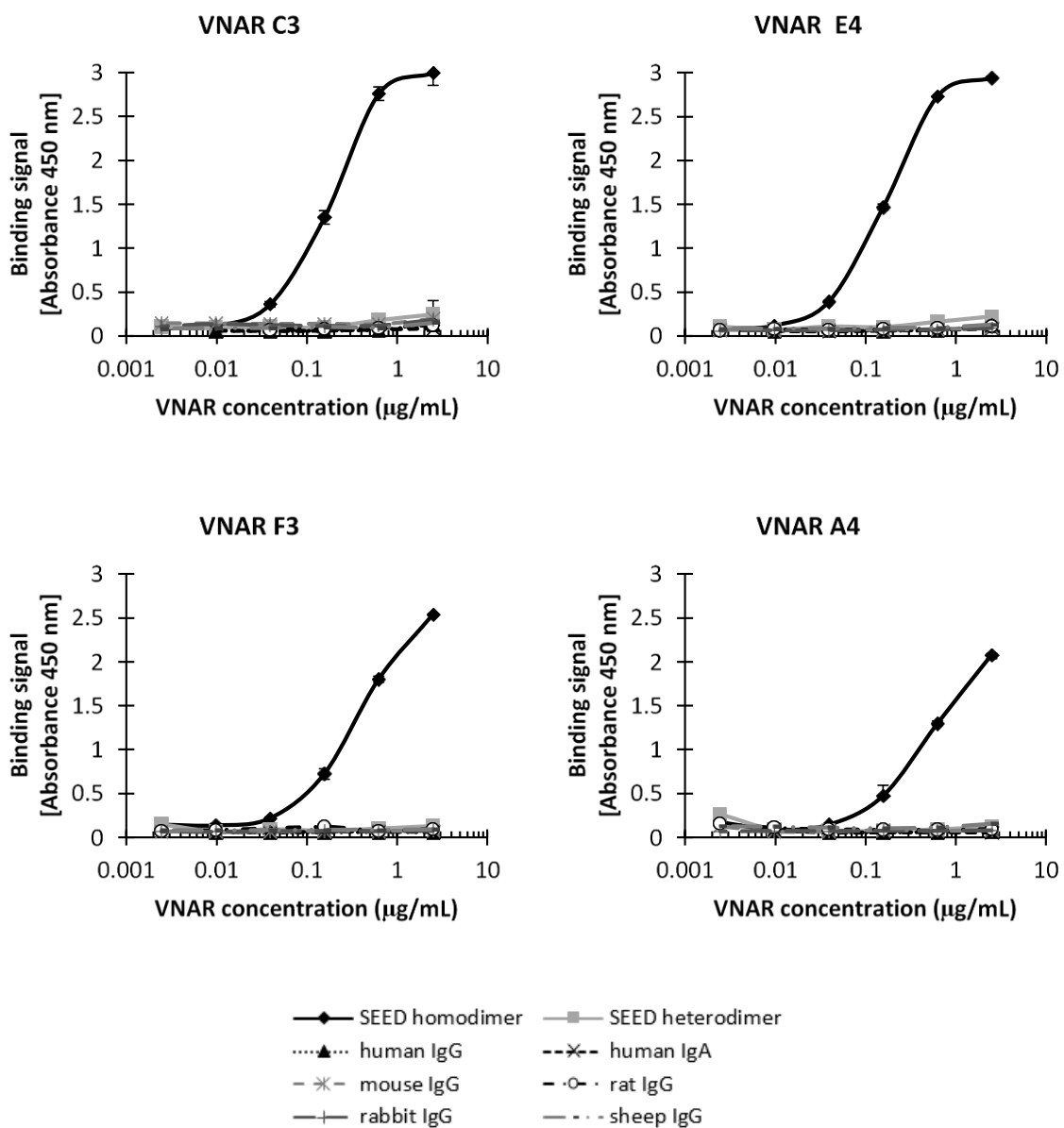
A



737

738 **Fig. 2.** Sequence analysis of selected VNAR leads. (A) Amino acid sequence alignment
 739 (clustalW) of selected anti-SEED homodimer VNAR leads, with dots indicating amino acid

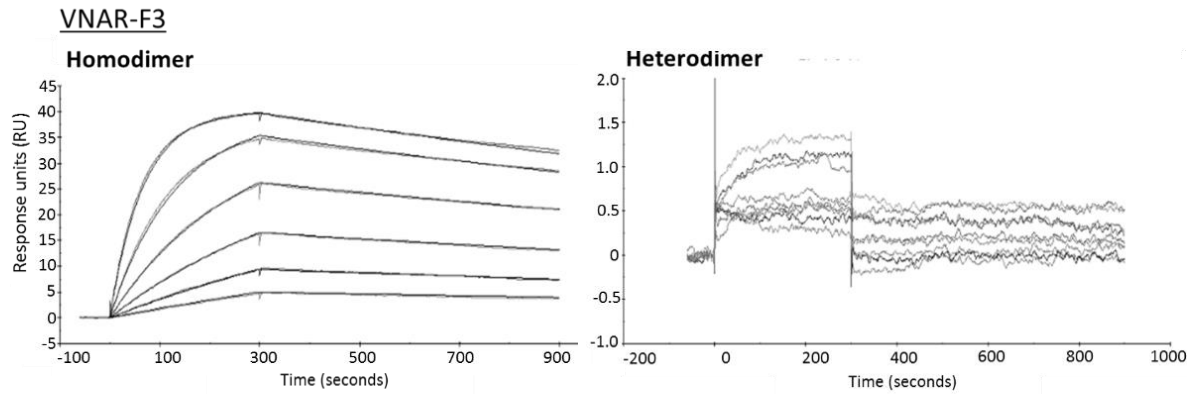
740 identity with the consensus (majority) sequence of the synthetic library backbone. Standard
 741 single letter amino acid nomenclature is employed. Relevant tags present: hexa-histidine tag -
 742 HHHHHH, c-Myc tag - EQKLISEEDL. **(B)** Ribbon representation of VNAR F3 domain
 743 generated *via* homology modelling using SWISS-MODEL and PyMOL software. VNAR F3
 744 domain modelled on PDB entry 4hgk (type IV short CDR3 loop) (Kovalenko *et al.* 2013).
 745 CDR1 and CDR3 loops, and the disulphide bond (S-S bond) formed between cysteine residues,
 746 are indicated. SWISS-MODEL accessed at <http://swissmodel.expasy.org/> and PyMOL
 747 software (Schrödinger, Inc.).



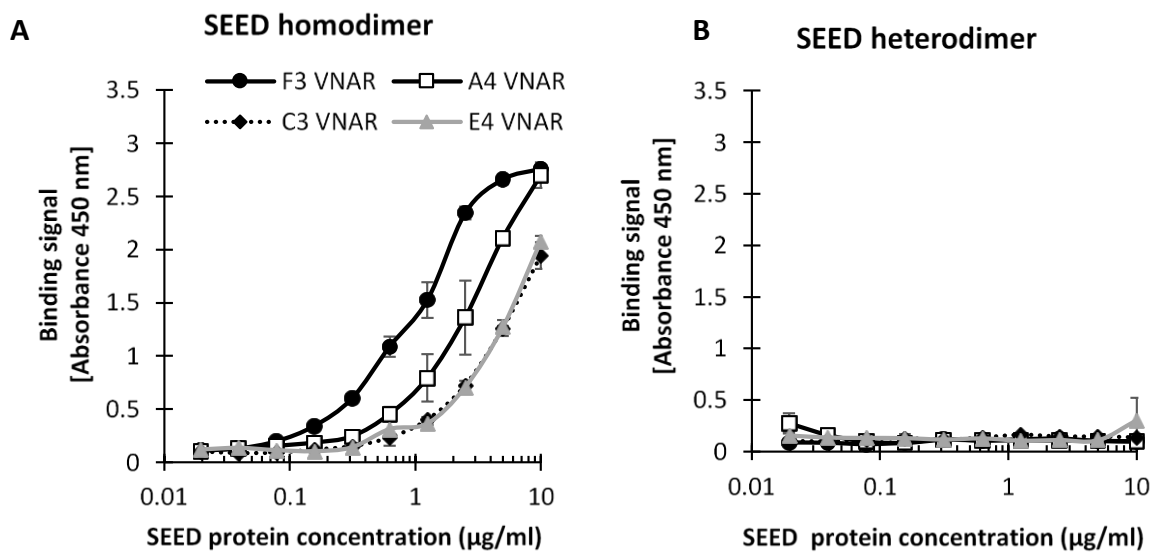
748

749 **Fig. 3.** Antigen-binding analysis of four VNAR proteins assessing selectivity to SEED

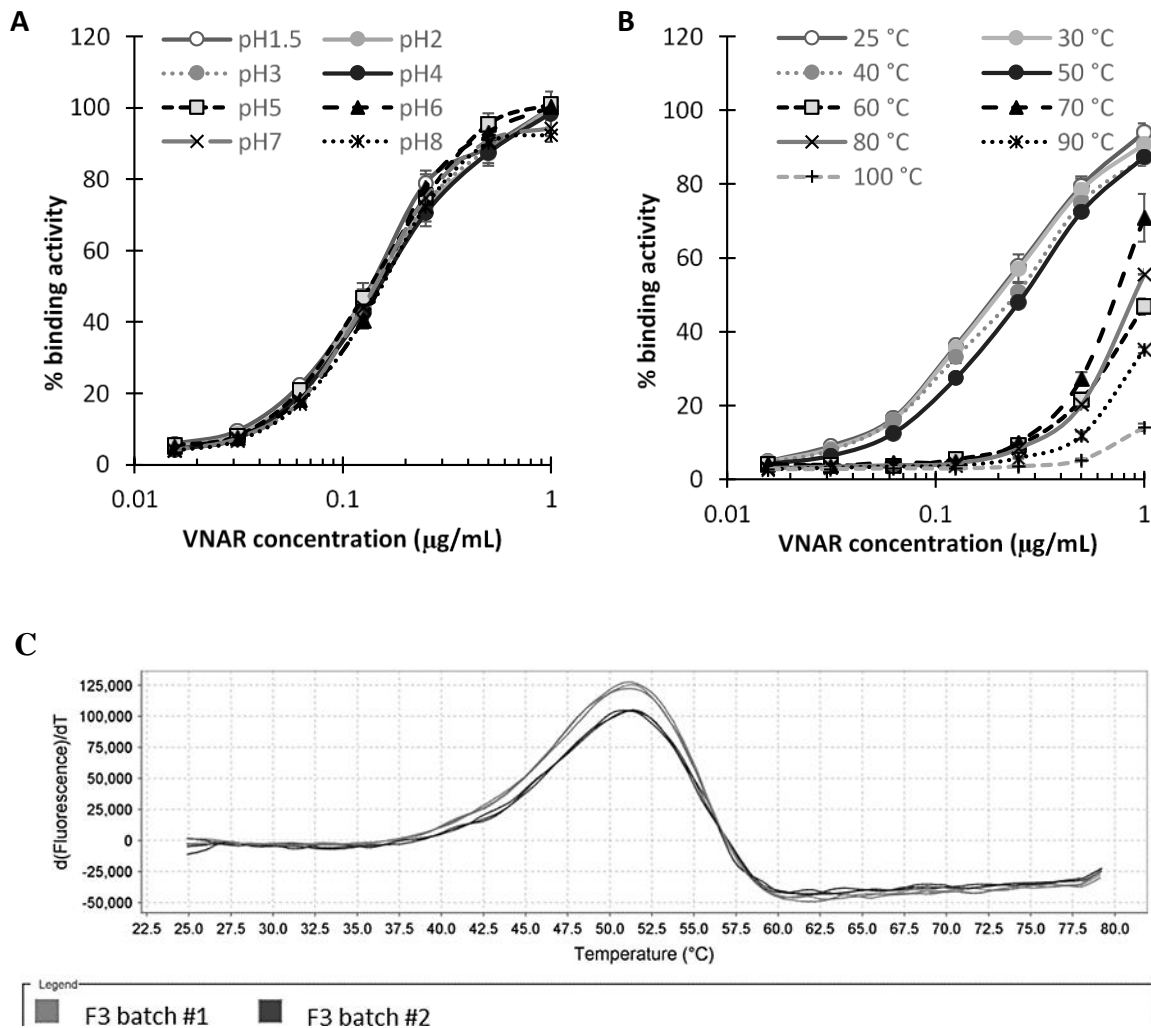
750 homodimer versus binding to analogue Fc scaffolds: SEED heterodimer, human IgG and IgA
751 from sera, and species cross reactivity to IgG from animal sera. Experiments were performed
752 in duplicate, standard deviations are indicated.



753
754 **Fig. 4.** BIAcore™ analysis of the F3 VNAR protein binding to SEED homodimer or
755 heterodimer coated CM5 chip. See Methods for protocol details.



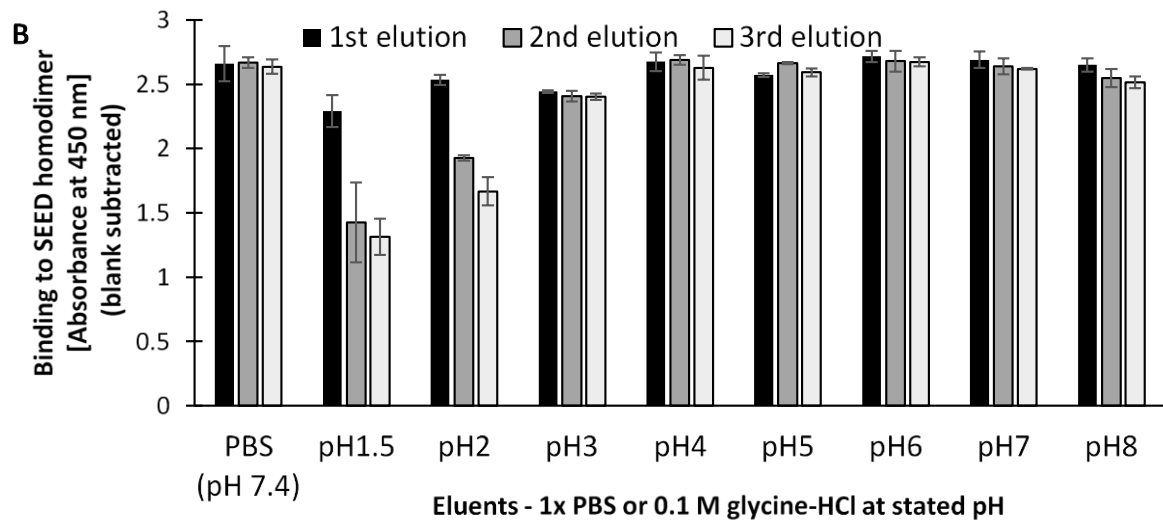
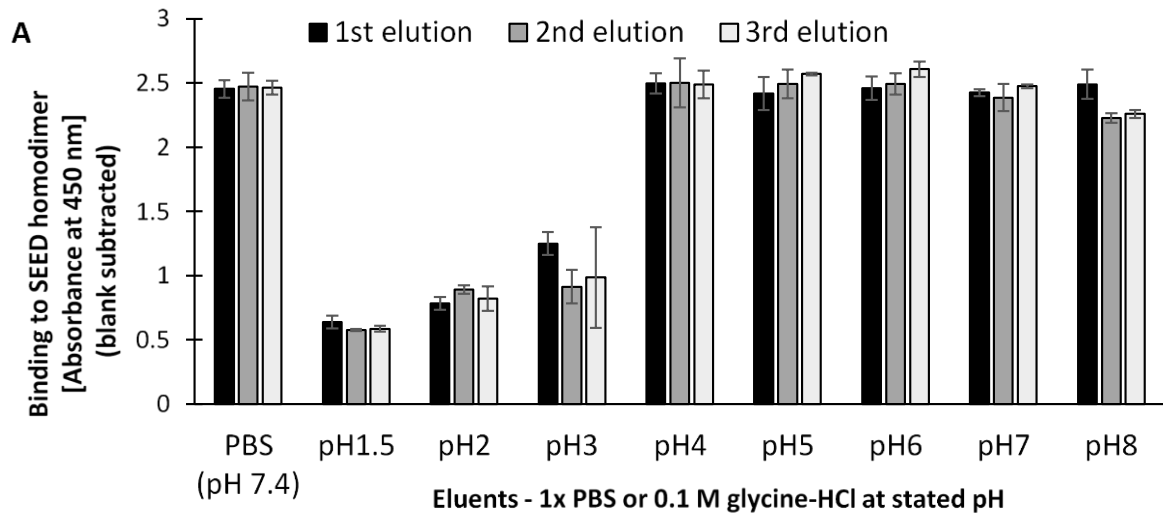
756
757 **Fig. 5.** Sandwich ELISA determining the activity of immobilised VNAR proteins as capture
758 reagents specific for SEED targets in solution. Either SEED homodimer (A) or SEED
759 heterodimer (B). Experiments were performed in duplicate, standard deviations are indicated.



760

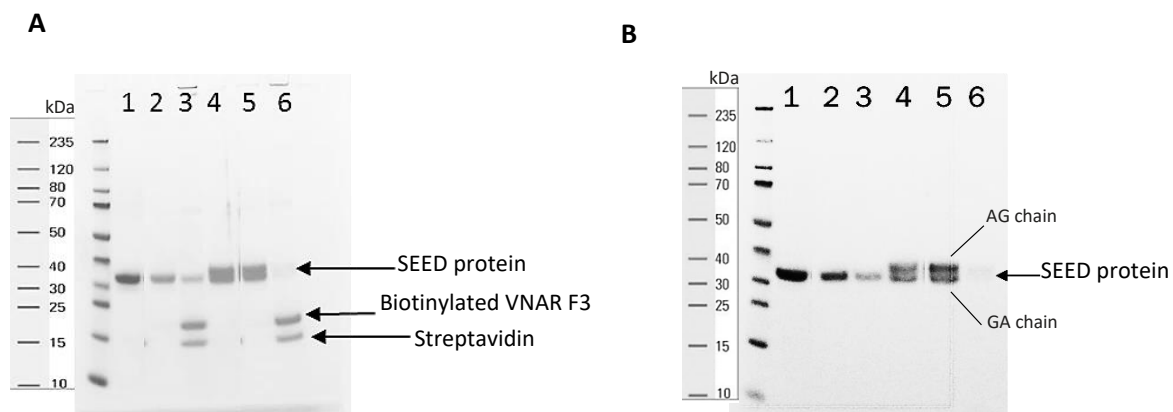
761

762 **Fig. 6.** Stability analysis of VNAR F3 protein to resist irreversible denaturation in a range of
 763 physiological and non-physiological conditions. The % binding activity to SEED homodimer,
 764 with respect to an untreated homodimer control, was determined following incubation at a
 765 range of (A) pH and (B) temperatures. Experiments were performed in duplicate, standard
 766 deviations are indicated. (C) Thermal shift assays determining T_m of VNAR F3 (two separate
 767 protein expression batches). Melt peaks are shown for each individual VNAR on the first
 768 derivative plot of fluorescence data. Experiments were performed in triplicate.



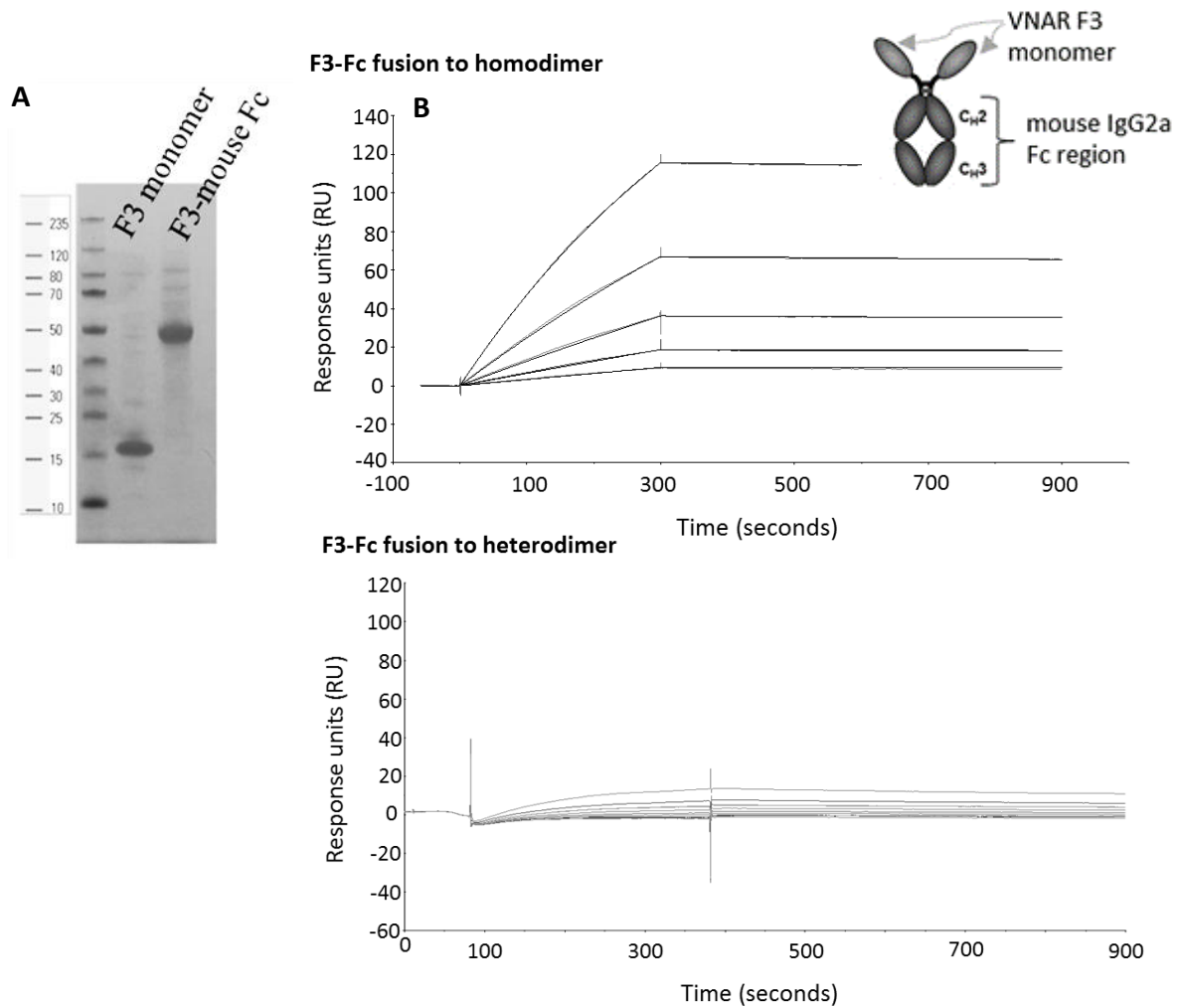
769

770 **Fig. 7.** ELISA-based elution assay comparing the effect of pH on elution efficiency.
 771 Absorbance values indicate relative amount of SEED homodimer bound to VNAR F3
 772 immobilised on an ELISA plate (A) upon application of eluents at various pH. Eluents were
 773 applied once, twice and three times. (B) Absorbance values indicate re-binding of immobilised
 774 VNAR F3 to SEED homodimer following multiple elutions at various pH. Experiments were
 775 performed in duplicate, standard deviations are indicated.



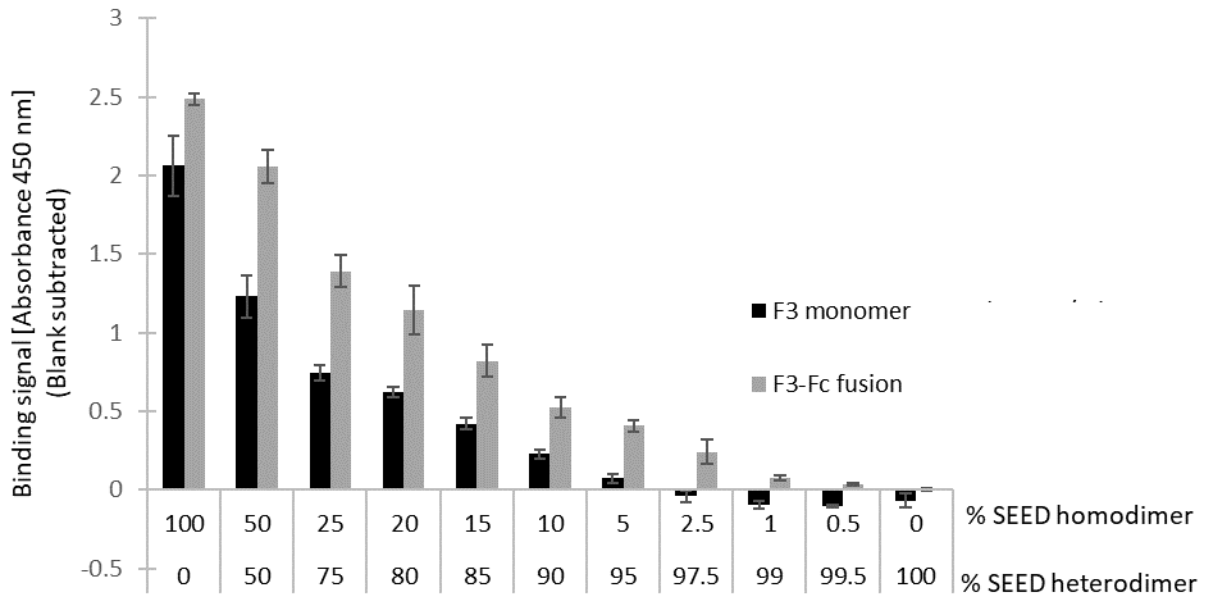
776

777 **Fig. 8.** Assessing capture of SEED protein *via* biotinylated VNAR F3 immobilised on
 778 streptavidin magnetic beads. SEED protein - either homodimer (lane 1) or heterodimer (lane
 779 4) prior to depletion (control), depleted supernatant (lane 2 and 5 respectively) and VNAR-
 780 functionalised streptavidin beads post-depletion (lane 3 and 6 respectively). **(A)** SDS-PAGE
 781 analysis of reduced samples detected with Coomassie staining. **(B)** Western blot analysis of
 782 reduced samples detected with anti-human IgG (Fc specific)-HRP conjugate. Protein marker:
 783 Spectra™ multicolour broad range protein ladder.



784

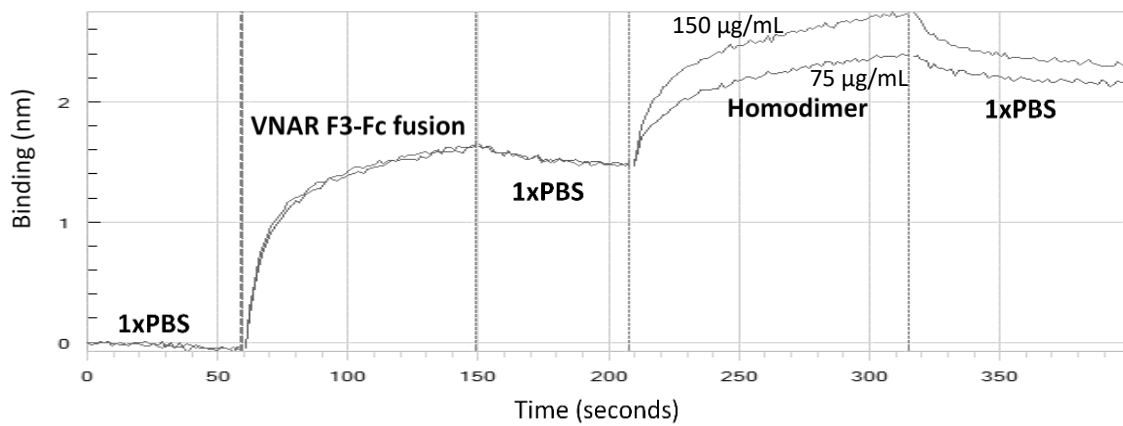
785 **Fig. 9.** Quality assessment of purified VNAR F3-Fc fusion. (A) SDS-PAGE of reduced
 786 samples, the VNAR F3-Fc fusion and a VNAR F3 monomer for comparison. (B) BIAcore™
 787 T200 Sensorgrams of the VNAR F3-Fc fusion used to determine K_D values *via* surface plasmon
 788 resonance. SEED homodimer or heterodimer protein was immobilised on the CM5 chip
 789 surface.



790

791 **Fig. 10.** Sandwich ELISA determining binding selectivity of the VNAR F3 monomer versus
 792 the F3-Fc fusion in a heterogeneous mix of SEED proteins in solution. SEED binding was
 793 detected with an anti-hIgG Fc-HRP. Experiments were performed in duplicate, standard
 794 deviations are indicated.

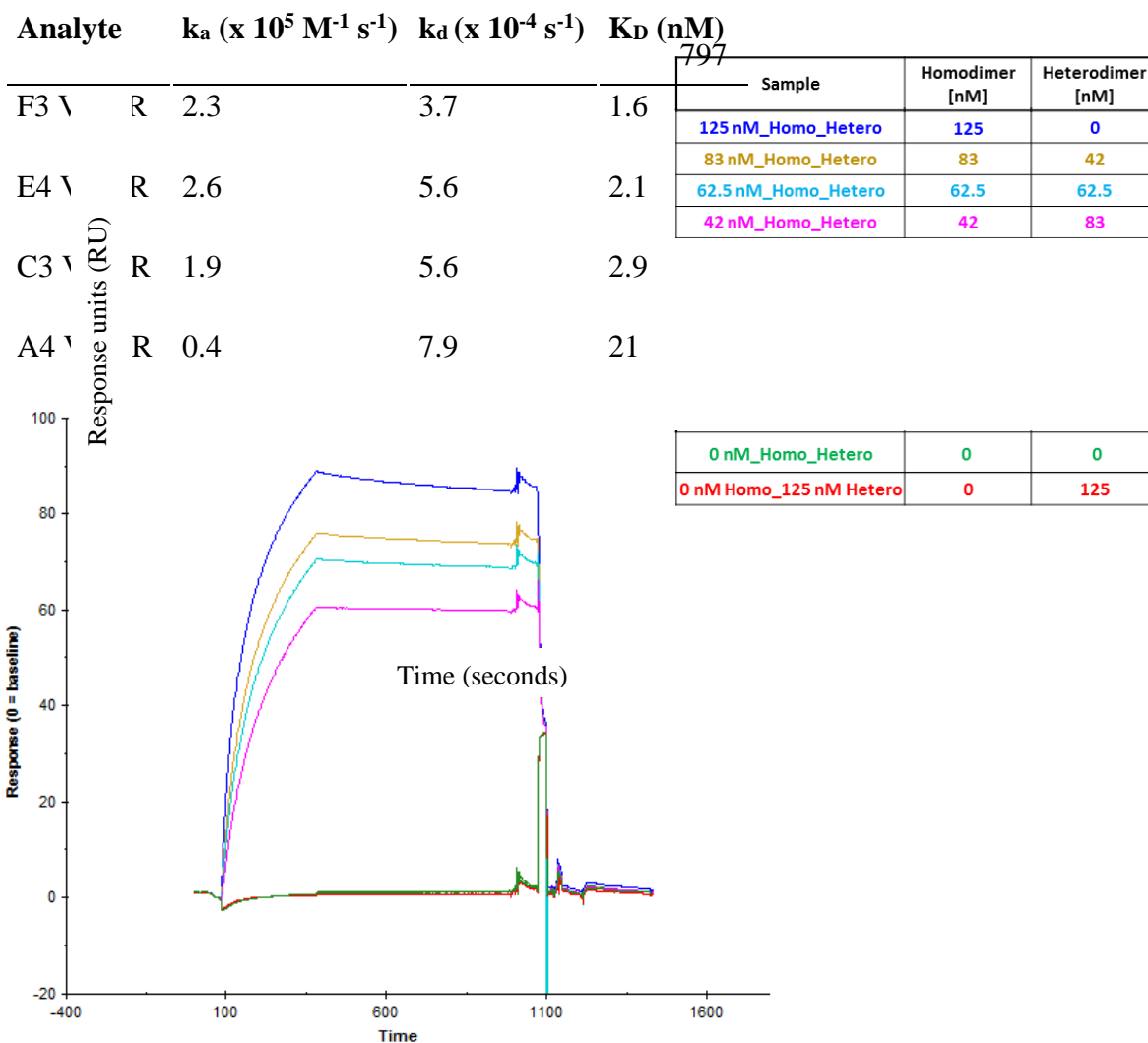
A



795

B

796



798

799 **Fig. 11.** Binding assessment *via* bio-layer interferometry on the Octet® QK System (Pall
800 FortéBio) and surface plasmon resonance on a BIAcore™ T200 System. (A) VNAR F3-Fc
801 fusion capture *via* anti-mouse IgG Fc and the detection of SEED homodimer in solution, with
802 concentration-dependent binding observed. (B) Surface plasmon resonance sensorgrams
803 depicting binding between amine coupled VNAR F3 on the chip surface (at 200 RU) and its
804 ability to recognise homodimer protein in a range of SEED protein mixtures. Response levels
805 shown are with background values subtracted, and 0 RU marking the baseline.

806 **Table 1.** Kinetic measurements of VNAR protein (analyte) binding to ligand SEED
807 homodimer. Association (k_a) and dissociation (k_d) rate constants, and the equilibrium
808 dissociation constants (K_D) shown. No binding to SEED heterodimer was observed for any of
809 the clones tested.

Analyte	k_a ($\times 10^5 \text{ M}^{-1} \text{ s}^{-1}$)	k_d ($\times 10^{-4} \text{ s}^{-1}$)	K_D (nM)
F3 VNAR	2.3	3.7	1.6

E4 VNAR	2.6	5.6	2.1
C3 VNAR	1.9	5.6	2.9
A4 VNAR	0.4	7.9	21

810

811 **Table 2.** Kinetic measurements of VNAR F3 monomer versus F3-Fc fusion (dimer) binding to
812 SEED homodimer ligand. Association (k_a) and dissociation (k_d) rate constants, and equilibrium
813 dissociation constants (K_D) shown. No binding to SEED heterodimer was observed (Figure 9).

Analyte	k_a ($\times 10^5 \text{ M}^{-1} \text{ s}^{-1}$)	k_d ($\times 10^{-4} \text{ s}^{-1}$)	K_D (nM) ⁸¹⁴
F3 monomer	1.9	3.0	1.5
F3-Fc	0.7	0.4	0.6